Performance Evaluation of Prequalified Steel Seismic Structural Systems in Canada

T.Y. Yang, M. Murphy & F. Lam
University of British Columbia, Vancouver B.C.

SUMMARY:
Performance-based earthquake engineering aims to measure the seismic performance of structures using metrics that are of immediate use to both engineers and stakeholders. A rigorous yet practical implementation of performance-based earthquake engineering methodology is presented. The methodology consistently accounts for the uncertainties in the hazards exposed by the structure, structural response and structural damage to quantify the performance of the entire system. A prototype office building designed according to the National Building Code of Canada was used to compare the seismic performance of six prequalified steel seismic force resisting systems. Both the material usage and the expected repair cost at different earthquake shaking intensities are presented in this paper. The outlined example demonstrates a clear and transparent procedure to compare the performance of different seismic force resisting systems and allows stakeholders to make an informed risk-based decision to select the best structural system.

Keywords: Seismic Design, Steel Structures, Braced Frame, Moment Frame, Performance based Design

1. INTRODUCTION

Structural steel is one of the most prevalent building materials used in North America. In seismically active regions, several different structural steel Seismic Force Resisting Systems (SFRS) have been developed. Some of the most commonly used systems are the Moment Resisting Frame (MRF), Concentrically Braced Frame (CBF), Eccentrically Braced Frame (EBF), Buckling Restrained Braced Frame (BRBF) and the Steel Plate Shear Wall (SPSW). Selection of the structural system is usually based on engineering judgment. The typical approach is to select a structural system which satisfies the minimum standard specified by the local building code(s) and which carries the minimum initial construction cost. The relative seismic performance of the system throughout its life cycle is not usually considered; total lifecycle costs include not only the initial construction cost but also the repair costs associated with probable earthquakes. In order to compare the performance of the MRF, CBF, EBF, BRBF and SPSW at different earthquake shaking intensities, a five story office building located in Vancouver, British Columbia, is designed. This building is designed with the assistance of a local Vancouver based structural engineering firm according to the requirements specified in the National Building Code of Canada (NBCC 2011) and Canadian Steel Code CSA S16-09 (CSA 2010). Per CSA S16-09 the MRF, BRBF, EBF and SPSW were designed as Type Ductile systems. For the CBF a type Moderately Ductile system was designed in addition to an X-braced frame (XBF) proportioned according to the Conventional Construction clause of the code. A detailed performance assessment of the prototype building using each of these systems was analysed using the performance-based assessment methodology presented by Yang et al. (2009a). This methodology uses a Monte-Carlo simulation procedure in which the building is analysed under numerous earthquake ground motions, with repair costs aggregated to determine rates at which different repair costs occur. To carry out the procedure, major structural and non-structural components of the buildings are identified and assigned to performance groups. Damage fragility relations, corresponding repair methods, repair material quantities and repair cost functions are defined for each performance group. Finite element models of the buildings were developed. Nonlinear dynamic analyses for individual earthquake ground motion records are conducted to establish peak response quantities. Based on the peak response, damage states of the components are identified using the fragility relations for each performance group. Repair cost is then calculated based on the building damage state. To generate cost statistics, the process is repeated a large number of times for different earthquake ground motion records. The results of the performance assessment are used to compare the relative performance of these six structural systems.

2. DESCRIPTION OF THE PROTOTYPE BUILDINGS

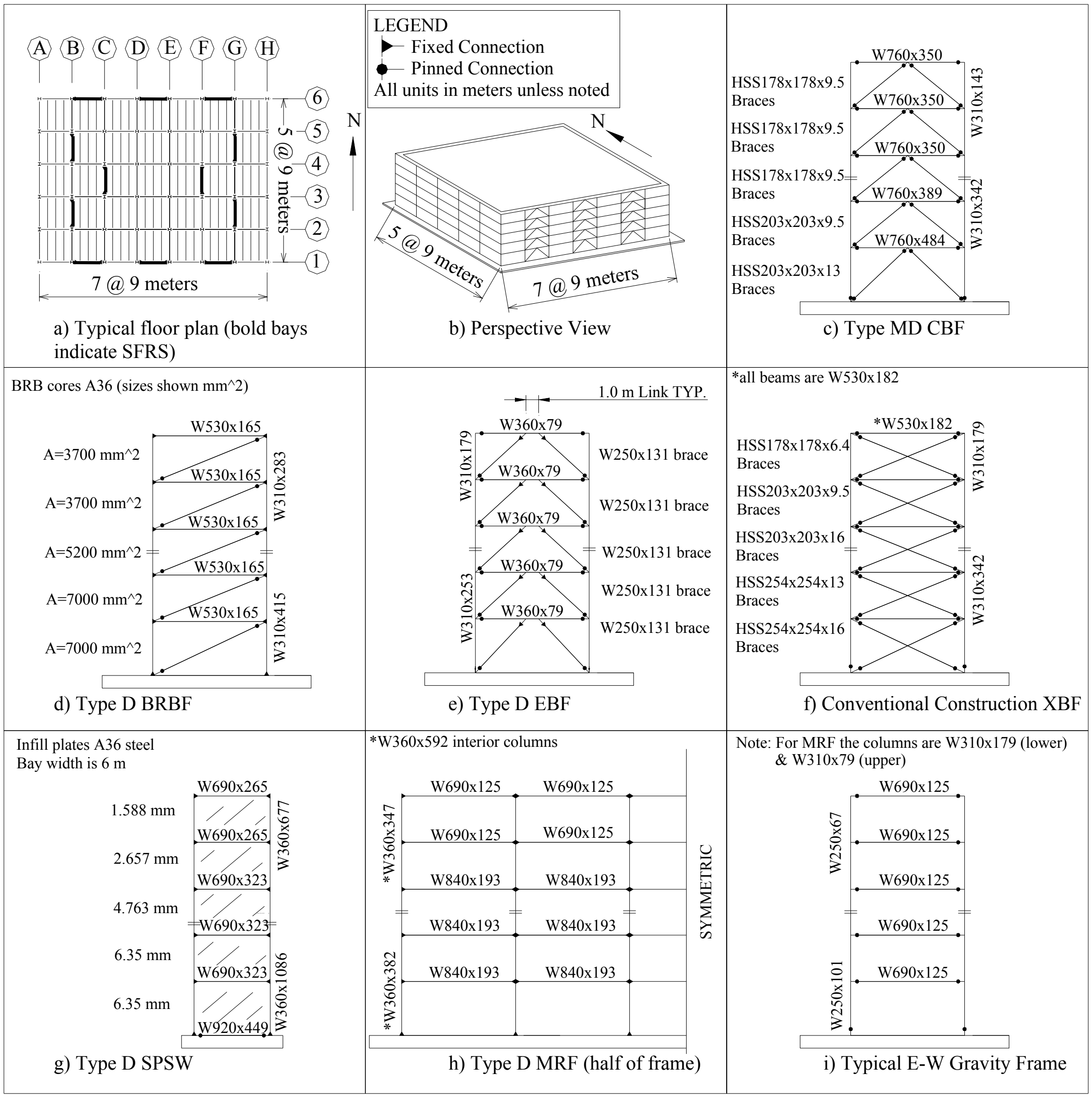

Figure 1. Summary of Structural Designs

A prototype five story (seven by five bays) office building without a basement level was selected for this study. The building has a bay width of 9 meters, a first story height of 4.25 meters and a floor height of 3.65 meters at other levels. The building is symmetric in both the North-South and East-West directions. Figure 1a shows a typical floor plan and 1b shows a perspective view of the structure. The SFRS bays are indicated in Figure 1a. All structural members were designed according to the National Building Code of Canada 2010 (NBCC 2010) and the Canadian Institute of Steel Construction design standard (CSA 2010). Six code prequalified SFRS are included in this study. These include a Type Ductile Moment Resisting Frame, a Type Ductile Eccentrically Braced Frame, a Type Ductile

Buckling Restrained Braced Frame, a Type Ductile Steel Plate Shear Wall, a Type Moderately Ductile Concentrically Braced chevron braced frame and a Conventional Construction Type X-Braced frame. Figures (c)-(h) show the detail of the SFRS bays for the different systems. The MRF and SPSW have slightly different arrangements than those of the braced frames. The MRF, shown in (h), is 5 bays long and is located at the perimeter of the structure, at bay lines A & H (North-South) and centred between two gravity bays along bay lines 1 & 6 (East-West). The SPSW is located centred at the perimeter of the building along bay lines B & G (North-South) and 1 & 6 (East-West). Figure 1i shows the configuration for the typical gravity bays. Note that gravity columns for the MRF structure are different because the columns were designed with a column effective length factor of K=1.2, whereas the gravity columns of the braced frames were designed with K=1.0. This reflects the ability of the gravity frame to sway laterally in the MRF. Also note that North-South gravity beams are W460x60 wideflange members.

3. PERFORMANCE GROUPS

Components of the building were assigned to 21 performance groups (PGs). These include: one structural PG at each floor level (1- 5), one exterior (6-10) and one interior (11-15) drift sensitive non-structural component PG at each floor, one interior acceleration sensitive non-structural component PG at each floor (16-20) and one elevator PG (PG 26). Performance group data is based on the PEER report by Moehle et al. (2011). PGs constitute building elements likely to be damaged and have costly repair actions associated with them after a seismic event. PGs are dependent on either interstory drift or story acceleration depending on which EDP causes damage to that element. For example, during an earthquake the lateral seismic resisting system is likely to sustain damage; damaged brace members will have a considerable replacement cost. Since brace damage is linked to interstory drift (rather than story acceleration), the structural PG is associated with this EDP as well as the costs associated with repair/replacement of braces. Since there are braces on every level, each floor has a structural PG whose repair cost is determined by its interstory drift. The non-structural components were divided into displacement and acceleration groups. Multiple damage states (DS) are defined for each PG, these states correspond to different levels of damage and the associated repair actions. For example, the exterior drift sensitive non-structural component performance group at the first floor (PG 6) has three states. States range from none (DS1) to minor (DS2) to severe damage (DS3). Whereas DS1 corresponds to no repair action necessary (no damage = $0 repair cost), DS2 corresponds to some repair and the associated costs, and DS3 corresponds to loss of the element, in which case it must be replaced (cost is that of replacement). For each state, a model (fragility relation) defines the probability of damage being less than or equal to the threshold damage given the value of the EDP associated with the PG. Figure 2 shows the fragility curves defined for PG 6. On this figure, if the interstory drift ratio is 1%, the PG has a 25% probability of being in DS2 and 75% probability in DS3; the probability of this PG being in DS1 is essentially 0%. Table 1 shows a summary of the performance groups included in this study. Symbols du_i and a_i represent the interstory drift ratio at the i^{th} story and the total floor acceleration at the i^{th} floor, respectively.

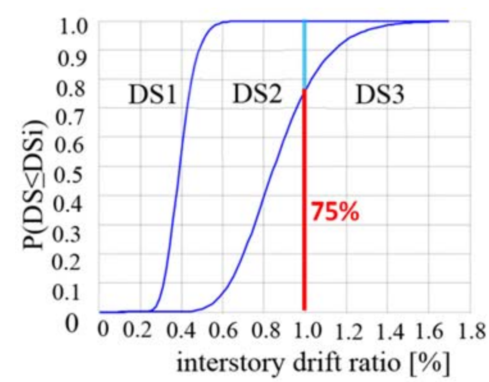

Figure 2. Example of fragility curves (Yang et al. 2009a)

Table 1. Summary of performance groups				
PG	Name	Location	EDP	Description
1	SH12	between levels 1 & 2	du1	
2	SH23	between levels 2 & 3	du2	structural system
3	SH34	between levels 3 & 4	du3	specific: based on
4	SH45	between levels 4 & 5	du4	replacement of braces,
5	SH5R	between levels 5 & R	du5	moment connections.ect
6	CW12	between levels 1 & 2	du1	
7	CW23	between levels 2 & 3	du2	
8	CW34	between levels 3 & 4	du3	Curtain Wall: based on
9	CW45	between levels 4 & 5	du4	repair/replacement of
10	CW5R	between levels 5 & R	du5	5'x6' exterior panels
11	INTD12	between levels 1 & 2	du1	
12	INTD23	between levels 2 & 3	du2	Interior nonstructural
13	INTD34	between levels 3 & 4	du3	drift sensitive:
14	INTD45	between levels 4 & 5	du4	partitions, doors,
15	INTD5R	between levels 5 & R	du5	glazing,etc
16	Ceiling2	below level 2	a2	
17	Ceiling3	below level 3	a3	Interior nonstructural
18	Ceiling4	below level 4	a4	acceleration sensitive:
19	Ceiling5	below level 5	a5	ceilings, lights,
20	CeilingR	below level R	aR	sprinkler heads, etc
21	Elevator	at level R	aR	2 elevators in building

4. FINITE ELEMENT MODELS

Finite element models of the building were created for each of the six systems. The models were developed using OpenSees (UCB 1997). Due to symmetric nature of the building, only half of it was modelled. For simplicity, only the response in the East-West direction is presented in this paper. A 2D model consisting of the frames in line 1, 2 and 3 (Figure 1a) is placed in series and tied together using multi-point constraints at each floor. The first 3 (of six) bays were placed next to each other, with the first bay carrying the SFRS and the other two interior bays carrying the majority of the gravity load. To model the stiffness and strength of the beam to column connections, all pin and moment resisting connections are modelled using the semi-rigid connections proposed by Astaneh-Asl (2005). Column rotational stiffness's were modelled based on the approach proposed by Fahmy et al. (1998). Behaviour of the buckling restrained braces was approximated by calibrating the hysteretic material in OpenSees to match test data presented by Merritt et al. (2003). Concentric braces were modelled based on the approach presented by Yang et al. (2009b) and calibrated to match the test data presented by Black et al. (1980). The shear link for the Eccentric Braced Frame was modelled by calibrating the Steel02 material in OpenSees to match the test data by Gulec et al. (2010). The behaviour of the steel infill plate was modelled by calibrating the Clough model in OpenSees to test match the data presented by Rezai (1999). Figure 3 shows the calibration of the braces and shear link to the test data. All other elements were modelled using the flexibility formulation nonlinear fiber cross section beam column elements in OpenSees. Masses were lumped at the nodes according to the tributary area. The P-Δ effect was accounted for using the corotational transformation in OpenSees (de Souza 2000, Filippou and Fenves 2004). Rayleigh damping of 2.5% was assigned to the first and third vibrational modes of each building. Table 2 shows the five vibrational periods of each structure.

Table 2. Model Periods						
	MRF	EBF	BRBF	CBF	SPSW	XBF
T1 (sec)	1.28	0.66	0.90	0.54	0.58	0.45
T2 (sec)	0.42	0.22	0.33	0.19	0.22	0.18
T3 (sec)	0.22	0.14	0.19	0.12	0.14	0.12
T4 (sec)	0.13	0.10	0.14	0.09	0.11	0.09
T5 (sec)	0.10	0.09	0.10	0.08	0.08	0.07

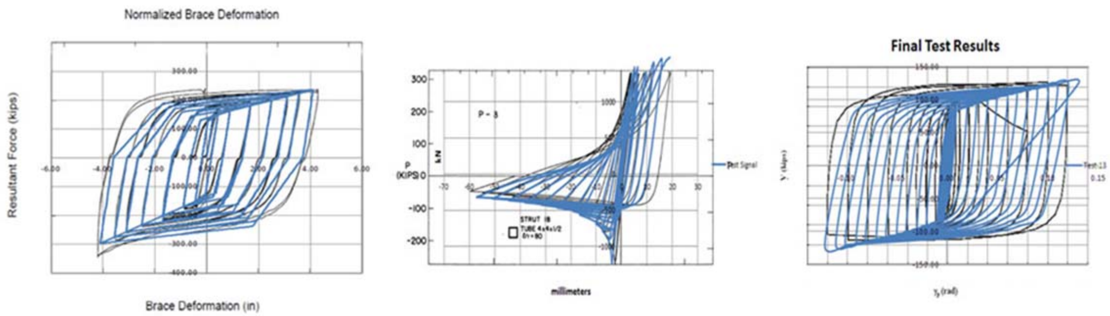

(a) BRB model (b) Concentric brace model (c) Shear link model

Figure 3. Calibration of element component models to test data

5. GROUND MOTION SELECTION

A detailed seismic hazard analysis was conducted for the building site in downtown Vancouver using the software package EZ-Frisk (Risk Engineering 2011). Using this program, a design spectrum was obtained for each hazard level of interest. Three hazard levels representing the 2% probability of exceedance in 50 years (2/50), 10% probability of exceedance in 50 years (10/50) and 50% probability of exceedance in 50 years (50/50) are included in this study. A total of 17, 18 and 16 ground motions were selected for the 2/50, 10/50 and 50/50 hazard levels, respectively. Motions were obtained from the PEER NGA database (PEER, 2011) and amplitude scaled to the target spectra. Ground motions were selected based on V_{s30}=360 to 760 m/s (Soil Class C). The ground motions were scaled such that the mean spectrum of the set of over the period range from $0.2T_{min}$ to $1.5T_{max}$ (where T_{min}=the smallest fundamental period of the 6 structures and T_{max} is the largest fundamental period) does not fall below 10% of the target spectrum. Figure 4 shows an illustrative example of the scaled spectra for the 2/50 hazard level. Table 3 lists the selected ground motions used in this study.

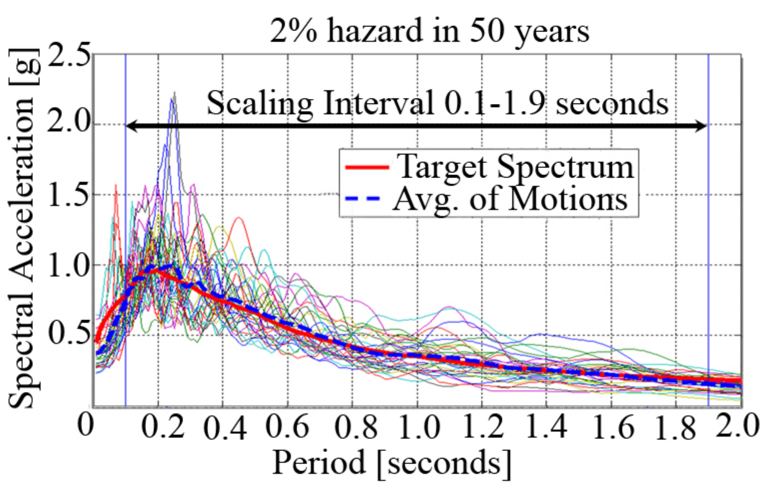

Figure 4. Ground motions scaled to 2% in 50 years target spectrum (both directions of each record shown)

Table 3. Ground Motions Selected for Time History Analysis					
2% in 50 Years Hazard Level		10% in 50 Years Hazard Level		50% in 50 Years Hazard Level	
Year	Event (Station)	Year	Event (Station)	Year	Event (Station)
1999	Chi-Chi-Taiwan(TCU089)	1999	Chi-Chi-Taiwan(TCU075)	1999	Chi-Chi-Taiwan(CHY088)
1989	LomaPrieta(Fremont)	1999	Chi-Chi-Taiwan(CHY088)	1999	Chi-Chi-Taiwan(TCU073)
1978	Tabas-Iran(Dayhook)	1978	Tabas-Iran(Dayhook)	1999	HectorMine(MillCreekStation)
2002	Denali-Alaska(PumpStation9)	1989	LomaPrieta(Fremont-Mission)	1978	Tabas-Iran(Dayhook)
1999	HectorMine(MillCreekStation)	2002	Denali-Alaska(TAPS Station9)	1989	LomaPrieta(Fremont-Mission)
1994	Northridge(Glendora-Oakbank)	1999	HectorMine(MillCreekStation)	1994	Northridge(Glendora-NOakbank)
1999	Chi-Chi-Taiwan(TCU078)	1994	Northridge(Glendora)	1983	Coalinga(Parkfield-StoneCorral)
1983	Coalinga(Parkfield)	1983	Coalinga(Parkfield)	2002	Denali-Alaska(TAPSStation9)
1976	Gazli-USSR(Karakyr)	1976	Gazli-USSR(Karakyr)	1999	HectorMine(Banning-TwinPines)
1979	Imp Valley-6(CerroPrieto)	1980	Irpinia-Italy(RioneroInVulture)	1979	ImperialValley(CerroPrieto)
1980	Irpinia-Italy(RioneroInVulture)	1979	ImpValley(CerroPrieto)	1980	Irpinia-Italy(RioneroInVulture)
1994	Northridge(Alhambra)	1980	Irpinia-Italy(Brienza)	1980	Irpinia-Italy(Brienza)
1980	Irpinia-Italy(Rionero)	1992	BigBear(RanchoCucamonga)	1994	Northridge(RanchoLosCerritos)
1989	LomaPrieta(GilroyArray6)	1994	Northridge(Alhambra-Fremont)	1992	BigBear(RanchoCucamonga)
1980	Victoria-Mexico(CerroPrieto)	1980	Victoria-Mexico(CerroPrieto)	1980	Victoria-Mexico(CerroPrieto)
1999	Kocaeli-Turkey(Goynuk)	1989	LomaPrieta(GilroyArray6)	1989	LomaPrieta(APEEL3EHayward)
1999	HectorMine(JoshuaTree)	1987	WhittierNarrows(PlayaDelRey)		
		1999	Kocaeli-Turkey(Goynuk)		

6. SEISMIC RESPONSE QUANTIFICATION

Nonlinear dynamic analyses were conducted to determine the seismic response of the buildings to each of the scaled ground motions. For each ground motion, the maximum of the EDP was recorded, and the median and standard deviation of these maxima are summarized in Tables 4, 5 & 6. Note that the MRF has the highest interstory drift (ISD), but the median of the maxima is less than the NBCC code limit of 2.5%. The maximum ISD for the MRF system was 2.5% (1^{st} level, 1994 NorthRidge ground motion). The XBF had the largest roof accelerations with a median of the maxima of 1.56g. The maximum roof acceleration the XBF experienced was 1.9g under the 1980 Irpinia Italy ground motion.

Table 4. Results for 2% in 50 years Hazard Level						
EDP [units]	EBF	CBF	BRBF	XBF	SPSW	MRF
du2 [%]	0.88(0.22)	0.48(0.12)	0.63(0.14)	0.33(0.07)	0.28(0.05)	1.43(0.45)
du3 [%]	0.35(0.13)	0.46(0.12)	0.49(0.14)	0.39(0.09)	0.3(0.04)	1.11(0.38)
du4 [%]	0.21(0.05)	0.51(0.11)	0.59(0.12)	0.33(0.06)	0.4(0.07)	0.93(0.22)
du5 [%]	0.18(0.02)	0.23(0.04)	0.6(0.11)	0.39(0.11)	0.63(0.12)	0.84(0.15)
duR [%]	0.1(0.02)	0.12(0.02)	0.34(0.06)	0.32(0.05)	0.52(0.15)	0.72(0.11)
ag [g]	0.36(0.1)	0.36(0.1)	0.36(0.1)	0.36(0.1)	0.36(0.1)	0.36(0.1)
a2 [g]	0.49(0.1)	0.61(0.14)	0.56(0.13)	0.61(0.14)	0.51(0.13)	0.53(0.09)
a3 [g]	0.41(0.09)	0.65(0.11)	0.56(0.11)	0.81(0.16)	0.53(0.12)	0.51(0.1)
a4 [g]	0.36(0.07)	0.7(0.09)	0.56(0.1)	0.96(0.16)	0.54(0.1)	0.51(0.11)
a5 [g]	0.41(0.06)	0.65(0.08)	0.55(0.07)	1.09(0.2)	0.58(0.07)	0.5(0.08)
aR [g]	0.6(0.1)	0.92(0.14)	0.82(0.13)	1.56(0.21)	0.82(0.1)	0.8(0.12)

Table 5. Results for 10% in 50 years Hazard Level						
EDP [units]	EBF	CBF	BRBF	XBF	SPSW	MRF
du2 [%]	0.4(0.1)	0.25(0.08)	0.33(0.08)	0.17(0.05)	0.21(0.03)	0.74(0.23)
du3 [%]	0.19(0.02)	0.27(0.05)	0.31(0.06)	0.2(0.06)	0.24(0.03)	0.57(0.19)
du4 [%]	0.17(0.02)	0.26(0.11)	0.34(0.07)	0.17(0.05)	0.28(0.04)	0.48(0.15)
du5 [%]	0.13(0.02)	0.18(0.02)	0.34(0.08)	0.2(0.06)	0.36(0.06)	0.44(0.12)
duR [%]	0.07(0.01)	0.08(0.01)	0.21(0.04)	0.17(0.05)	0.32(0.04)	0.38(0.09)
ag [g]	0.19(0.05)	0.19(0.05)	0.19(0.05)	0.19(0.05)	0.19(0.05)	0.19(0.05)
a2 [g]	0.32(0.07)	0.35(0.07)	0.32(0.07)	0.34(0.07)	0.33(0.08)	0.29(0.05)
a3 [g]	0.27(0.07)	0.48(0.07)	0.32(0.07)	0.48(0.09)	0.39(0.08)	0.28(0.05)
a4 [g]	0.27(0.04)	0.5(0.13)	0.3(0.07)	0.51(0.12)	0.42(0.06)	0.27(0.06)
a5 [g]	0.3(0.04)	0.53(0.08)	0.33(0.06)	0.58(0.15)	0.45(0.07)	0.27(0.06)
aR [g]	0.42(0.08)	0.64(0.1)	0.51(0.1)	0.83(0.22)	0.67(0.07)	0.42(0.08)

Table 6. Results for 50% in 50 years Hazard Level						
EDP [units]	EBF	CBF	BRBF	XBF	SPSW	MRF
du2 [%]	0.14(0.05)	0.08(0.03)	0.13(0.03)	0.07(0.02)	0.1(0.02)	0.28(0.09)
du3 [%]	0.12(0.03)	0.09(0.03)	0.12(0.03)	0.08(0.02)	0.12(0.02)	0.21(0.07)
du4 [%]	0.1(0.02)	0.09(0.03)	0.13(0.03)	0.07(0.02)	0.14(0.02)	0.18(0.05)
du5 [%]	0.08(0.02)	0.07(0.02)	0.13(0.03)	0.08(0.02)	0.19(0.03)	0.17(0.05)
duR [%]	0.04(0.01)	0.03(0.01)	0.08(0.02)	0.07(0.02)	0.17(0.02)	0.14(0.04)
ag [g]	0.07(0.02)	0.07(0.02)	0.07(0.02)	0.07(0.02)	0.07(0.02)	0.07(0.02)
a2 [g]	0.13(0.03)	0.13(0.03)	0.13(0.03)	0.13(0.02)	0.12(0.03)	0.1(0.02)
a3 [g]	0.14(0.03)	0.17(0.04)	0.12(0.03)	0.18(0.04)	0.16(0.03)	0.1(0.02)
a4 [g]	0.14(0.03)	0.17(0.05)	0.12(0.03)	0.2(0.05)	0.16(0.03)	0.1(0.02)
a5 [g]	0.17(0.04)	0.19(0.05)	0.13(0.03)	0.22(0.06)	0.19(0.04)	0.1(0.02)
aR [g]	0.21(0.04)	0.24(0.05)	0.19(0.04)	0.31(0.08)	0.27(0.06)	0.16(0.03)

*Table 4, 5 & 6 are the median of maximum values (standard deviation)

7. COMPUTE THE REPAIR COSTS

The response presented in Tables 4 to 6 were used in a mathematical model to statistically generate a large numbers of additional maxima having the same statistical properties as the original set. Details for this procedure are presented in Yang et al. (2009a). The damage state is determined using the EDP and the fragility curve together with a random number generator varying from 0 to 1.0 to determine the ordinate (Figure 2). The damage state, together with the repair quantity (number of ceiling tiles per floor, for example) and the unit repair cost determines the cost associated with the PG. The costs for each PG are summed for the entire building. This procedure is then repeated several thousand times; the details of this procedure are given in Yang et al. (2009a). Because the repair cost has a statistical distribution, the result of this analysis is a cumulative distribution function. Figure 5 (a)-(c) shows the discrete cumulative distribution functions of the total repair costs for the six systems at each of the three hazard levels considered. The repair cost and the seismic hazard relations can be combined to determine the mean annual rate of the repair cost exceeding a threshold value. This result is obtained by first computing the complement of the cumulative distribution function, then multiplying it by the slope of the hazard curve at the corresponding ground motion intensity level, and finally integrating the resulting curves across the seismic hazard interval considered in the seismic hazard analysis. Repeating this process for all repair cost values produces a loss curve that represents the mean annual rate of the repair cost exceeding a threshold value. The area under this loss curve represents the mean annualized total repair cost. Details of this procedure are given in Yang et al. (2009a). Figure 6d shows the loss curve for the CBF frame system; integration of the area under this curve yields a value of $53,400; this value has relevance to the premium one would be willing to pay to insure the building against the repair cost of future earthquakes.

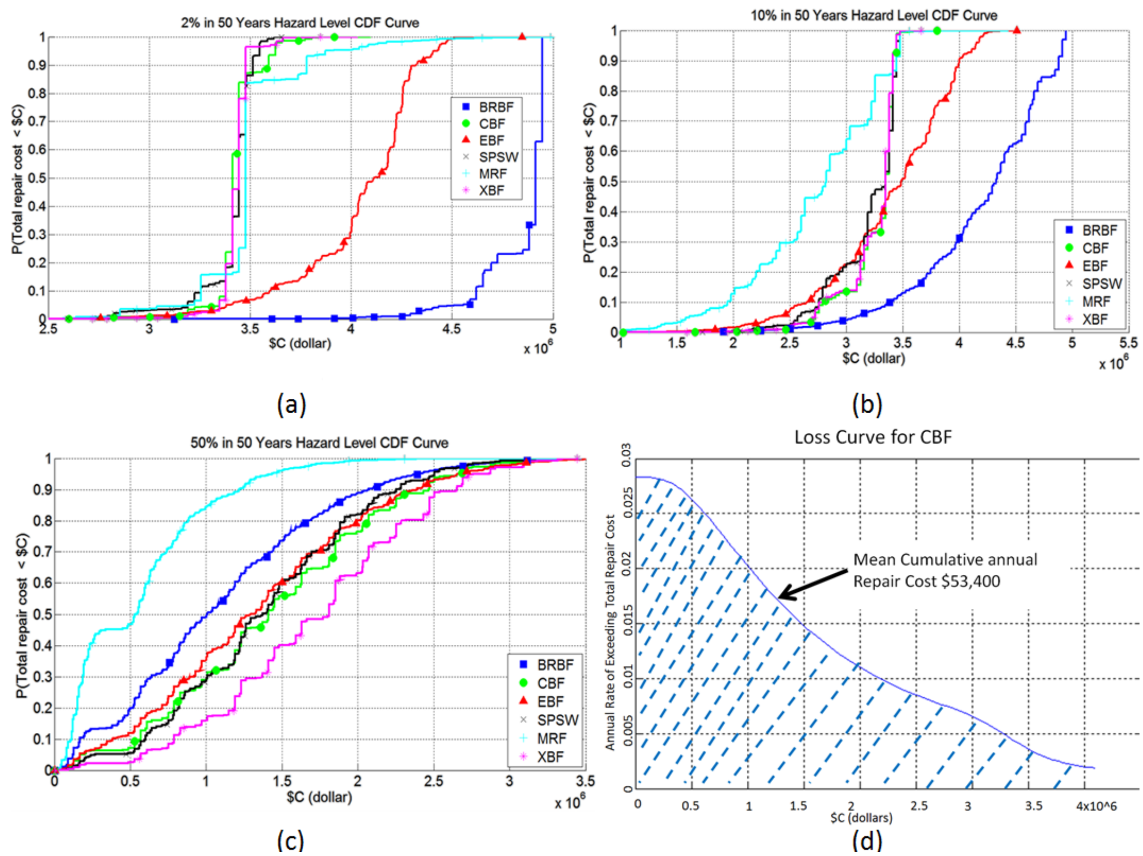

Figure 5. Discrete CDF of repair cost distribution (a-c), Loss Curve for CBF (d)

Table 7 shows a summary of the total building weight and median repair cost of each system. For comparison, the structural steel usage (including the gravity members) is compared with the heaviest system, the MRF. The material usage comparison shows that the EBF uses the least steel. The median repair cost taken at the 50% probability value of the CDF curves (shown in Figure 6 a-c) indicates that the CBF has the lowest median cost at the 2/50 hazard level. Finally, the mean cumulative annual repair cost of each structure shows that the BRBF appears to be a very economical system, carrying both the second lowest annual repair cost and the second lowest usage of structural steel. The MRF system carries the lowest repair cost by far, but it uses the greatest amount of material. Although connection costs will be significant, overall structural steel usage is considered an indicator of building initial construction cost. It is possible to look at the breakdown of costs for each system at a given hazard level. Figure 6 shows that for the BRBF system at the 2/50 hazard level most of the costs result from the ceiling components (PG 16-20) and the structural performance group (PG 1-5). Note that the BRBF median repair cost is considerably lower at the 50/50 Vs. the 2/50 hazard level. This is because the structural performance group for the BRBF only has two states, DS1 or DS2 corresponding to the braces either being undamaged or having failed and needing replacement. At the lowest level of seismic shaking the braces are undamaged and this PG does not contribute significantly to the repair cost at all. The five other systems have 4 structural damage states compared to the BRBF’s two; this is the primary reason why the median repair cost is so much higher for the BRBF at the 2/50 hazard level. If the BRBFs braces become damaged, they must be replaced; at lower levels of shaking however its SFRS system is undamaged. By comparison, the damage sustained by the other systems is more variable.

Table 7. Costs Associated with Different Steel Structural Systems							
	Usage. (kg)	Compare to MRF	Median Repair Cost from CDF 2/50	10/50	50/50	Annual repair Cost	Compare to XBF
MRF	702897	100%	$3,480,000	$2,820,000	$ 538,000	$ 30,900.00	51%
CBF	682403	97%	$3,410,000	$3,350,000	$ 1,410,000	$ 53,400.00	88%
SPSW	601896	86%	$3,440,000	$3,350,000	$ 1,370,000	$ 50,500.00	83%
BRBF	604979	86%	$4,910,000	$4,330,000	$ 1,000,000	$ 49,100.00	81%
XBF	591510	84%	$3,440,000	$3,350,000	$ 1,810,000	$ 60,600.00	100%
EBF	561057	80%	$4,110,000	$3,490,000	$ 1,290,000	$ 52,500.00	87%

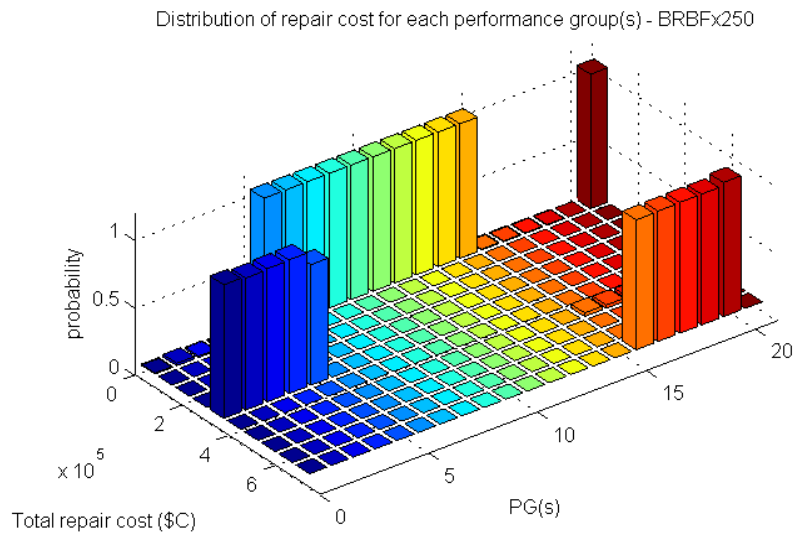

Figure 6. Distribution of cost for the BRBF building at 2% in 50 years hazard level

8. SUMMARY AND CONCLUSIONS

This paper presents a detailed performance assessment of a five-story office building designed using six prequalified structural steel systems in Canada. Although the less ductile systems were not included in this study (limited ductility CBF, limited ductile SPSW.ect), this analysis serves as a comparison of the different types of steel lateral SFRS used in industry and which are prequalified for use in Canada. Material element models were calibrated to test data so that the EDP would be as accurate as possible. The purpose of the investigation was to understand the relative seismic performance of these systems by comparing the initial material use and the post-earthquake repair costs at different levels of shaking intensity. The results provide a quantitative measure for engineers and other stake holders to make an informed decision to select the best system to achieve their design objective. The advent of the performance-based earthquake engineering methodology presented here offers important selection criteria in which the potential seismic economic loss of the facility is evaluated. Under the circumstances presented, the buckling restrained braced frame offers the second lowest material usage and the second lowest expected annual repair cost. Conclusions regarding the relative merits of these systems are somewhat anecdotal and may vary when the configurations of the structure are changed. The accuracy of the loss analysis depends heavily on the accuracy of the fragility and associated cost data. However, the overall methodology presented is widely applicable and offers a quantitative measure which can be used by engineers to make informed decisions in selecting the best structural system for a given project.

ACKNOWLEDGEMENTS

This work was funded in part by the Natural Sciences and Engineering Research Council of Canada (NSERC) jointly with the Steel Structures Education Foundation (SSEF), award reference number 150656511 (application ID 411465). The authors would like to acknowledge David MacKinnon of the SSEF for making this project possible. The authors would also like to thank: Dr. Didier Pettinga, P.Eng and Rob Simpson, P.Eng of Glotman Simpson Consulting Engineers for their help designing the prototype models; Members of the ATC-58 project team for providing fragility, repair method and repair cost information for the performance groups used in this study. Any opinions, findings and conclusions or recommendations expressed in this material are those of the authors and do not necessarily reflect those of the Natural Sciences and Engineering Research Council of Canada or the Steel Structures Education Foundation.

REFERENCES

Astaneh-Asl, A. 2005. "Design of shear tab connections for gravity and seismic loads," SteelTips, Structural Steel Educational Council.

ATC. 2007. "Development of next generation performance-based seismic design procedures for new and existing buildings," Applied Technology Council, Redwood city, CA. http://www.atcouncil.org/atc-58.shtml

Black, Wenger & Popov, (1980). "Inelastic buckling of steel struts under cyclic load reversals," Report to sponsors at the National Science Foundation and the American Iron and Steel Institute, University of California at Berkeley, Report No. UCB/EERC-80/40

Cochran, Michael & Honeck, William, 2004. "Design of Special Concentric Braced Frames," SteelTips, Structural Steel Education Council

CSA S16-09. 2010. "Handbook of Steel Construction," Canadian Institute of Steel Construction, Markham, Ontario

de Souza, R.M. 2000. "Force-based finite element for large displacement inelastic analysis of frames," Doctoral dissertation, Graduate Division of the University of California, Berkeley.

EZ-Frisk, Risk Engineering Inc. (2011). http://www.riskeng.com/

Fahmy, Stojadinovic, Goel & Sokol. (1998), "Seismic behaviour of moment resisting steel column bases". 11th European Conference on Earthquake Engineering, Rotterdam

Filippou, F.C. & Fenves, G.L. 2004. "Methods of analysis for earthquake-resistant structures," Chapter 6 in Earthquake Engineering From Engineering Seismology to Performance-based Engineering, RCR Press, Boca Raton, Florida.

Gulec, Gibbons, Chen, Whittaker (2010), "Damage states and fragility functions for w-shape steel link beams in eccentrically braced frames," report to the Applied Technology Council for project ATC-58

López, Walterio & Sabelli, Rafael 2004. "Seismic Design of Buckling-Restrained Braced Frames," SteelTips, Structural Steel Educational Council

Merritt, Uang & Benzoni 2003. "Subassemblage Testing of Star Seismic Buckling-Restrained Braces", Structural Systems Research Project, University of California at San Diego, Report No. TR-2003/04

Moehle, Bozorgnia, Jayaram, Jones, Rahnama, Shome, Tuna, Wallace, Yang and Zareian (2011), "Case Studies of the Seismic Performance of Tall Buildings Designed by Alternative Means," PEER Report No. 2011/05, Pacific Earthquake Engineering Research Center, University of California Berkeley, CA

NBCC 2010, "National Building Code of Canada", National Research Council Canada, Ottawa, ON

Pacific Earthquake Engineering Research Center (PEER) Strong Motion Database 2011. University of California at Berkeley http://peer.berkeley.edu/peer_ground_motion_database

Rezai (1999), "Seismic behaviour of steel plate shear walls by shake table testing," doctoral dissertation at the University of British Columbia

UCB 1997. "Open system for earthquake engineering simula-tion (OpenSees) framework," Pacific Earthquake Engineering Research Center, University of California, Berkeley, http://opensees.berkeley.edu/.

Yang, T.Y., Moehle, J., Stojadinovic, B. & Der Kiureghian, A. 2009a. "Performance evaluation of structural systems: theory and implementation," Journal of Structural Engineering, ASCE. Vol. 135, No. 10, pg. 1146 – pg 1154

Yang, T.Y., Moehle. J. & Stojadinovic, B. 2009b. "Performance evaluation of innovative Steel Braced Frames," PEER report, Pacific Earthquake Engineering Research Center, University of California, Berkeley. Report number 2009/103.

Yang, T.Y., Bozidar Stojadinovic and Jack Moehle. "Demonstration of a practical method for seismic performance as-sessment of structural systems," Earthquake Spectra, EE-RI. (accepted for publication).